Scientific Research and Essays Vol. 6(22), pp. 4826-4838, 7 October, 2011
Available online at http://www.academicjournals.org/SRE
DOI: 10.5897/SRE11.1244
ISSN 1992-2248 ©2011 Academic Journals

Full Length Research Paper

Numerical investigation of laminar and turbulent mixed convection in a shallow water-filled enclosure by various turbulence methods

Mohammad Reza Safaei[1]*, Hamid Reza Goshayeshi[2], Behzad Saeedi Razavi[3] and Marjan Goodarzi[4]

[1]Department of Mechanical Engineering, Mashhad Branch, Islamic Azad University and Young Researchers Club, Mashhad, Iran.
[2]Department of Mechanical Engineering, Mashhad Branch, Islamic Azad University, Mashhad, Iran.
[3]Institute of Standard and Industrial Research of Iran, Khorasan Razavi, Mashhad, Iran.
[4]Department of Computer Engineering, Mashhad Branch, Islamic Azad University, Mashhad, Iran.

Accepted 16 August, 2011

In this study, we first modeled laminar mixed convection inside rectangular enclosure with moving wall and 'aspect ratio' = 10 and then the results were compared with other investigators. After showing verity of results, we continued our investigation with turbulent flow using standard $k-\varepsilon$, RNG $k-\varepsilon$ and RSM models for Richardson numbers 0.1 to 10 and Ra = 6 × 10^9. The results showed that the turbulence intensity depends on the position. For example, in vertical walls and boundary layer, the flow was laminar and flow in center of enclosure was turbulent. In addition, the results indicated that as the Richardson number increased, the velocity changed happen more frequently in the vertical direction and fluctuations were seen more and more. Another conclusion to be drawn was that at natural convections, the Reynolds stresses curves gone under too many fluctuations all of which was the great impact of the 'buoyancy force' and the properties of 'natural convection' within this Richardson number. The last and foremost deduction was that at the 'turbulence flow', 'heat transfer' was generally greater than laminar flow and that was due to high level of mixing at the first.

Key words: Reynolds stress, Richardson number, Boussinesq approximation, mixed convection heat transfer, turbulent intensity.

INTRODUCTION

Mixed convection heat transfer is a phenomenon in which both natural and forced convections happen. Mixed convection heat transfer takes place either when buoyancy effect matters in a forced flow or when there are sizable effects of forced flow in a buoyancy flow. Dimensionless numbers to determine this type of flow are as follows: Grashof number ($Gr = g.\beta.\Delta T.L^3/\nu^2$), Reynolds number ($Re = \rho.v.l/\mu$), Rayleigh number ($Ra = Gr.Pr$), Prandtl number ($Pr = C_p.\mu/K$) and Richardson number (Ri). If you divide natural convection effect by forced convection effect, it yields to Richardson number and it is written as such: $Ri = Gr/Re^2$. When it comes to limits and we have $Ri \rightarrow 0$ or $Ri \rightarrow \infty$, forced convection and natural convection become dominant heat transfers respectively (Safaiy and Goshayeshi, 2011). Mixed convection heat transfer is a fundamentally significant heat transfer mechanism that occurs in selection industrial and technological applications. Fluid flow and heat transfer in rectangular or square cavities driven have been studied extensively in the literature. A review shows that there are two kinds of studies: one way includes the entry of hot (or cold) fluid from one side, passing isothermal walls and exit from the other side. In this case, we could evaluate and compare the forced convection effect caused by the entry and exit of the fluid. Some

*Corresponding author. E-mail: CFD_Safaiy@yahoo.com. Tel: +98 9151022063.

scientists have applied thermal flux on the way fluid passes through the channel and then, they studied the effects of it. Among the studies, we can mention the ones done by Rahman et al. (2007), Saha et al. (2006, 2008). Another method to create mixed convections is to move enclosure walls in presence of hot (cold) fluid inside the enclosure. This creates shear stresses and provides thermal and hydrodynamic boundary layers in the fluid inside the enclosure and eventually creates forced convection in it. Numerous studies have been conducted in this field so far. We can mention the study done by (Oztop and Dagtekin, 2004) as an instance. They have studied a two-dimensional square shaped enclosure with vertical isothermal moving walls and insulated horizontal walls. In this work, different situations have been considered concerning the movement of vertical walls and $0.01 \leq Ri \leq 100$ have been presupposed. The rate of heat transfer has also been expressed in the form of Nusselt numbers. The results of this work suggest that in low Richardson values, if the moving walls move in the opposite directions, heat transfer from enclosure is more than when walls slide convergent.

Basak et al. (2009) studied the mixed convection flow inside a square enclosure with left and right cold walls, insulated moving upper wall and fixed lower hot wall by using finite element method. They suggested that by increasing Gr with Pr and Re fixed, recirculation power would improve. In 2007, Sharif (2007) studied the 'laminar mixed convection' in inclined rectangular enclosures with aspect ratio of 10 by using Fluent 6. He let the Rayleigh number variable to be between 10^5 to 10^7 and Reynolds number fixed to be 408.21. The fluid he used was water with Prandtl as 6 and the enclosure inclination angel to the horizon varied between 0° to 30°. The mentioned enclosure had hot moving upper wall, cold fixed lower wall and adiabatic left and right walls. His study showed that local Nusselt number heightened by increasing the enclosure's inclination angel. It is undeniable that the advancement in different sciences in the last decade has resulted in much subtle laboratory measuring tools and it is true that using of modern methods like parallel processing has enabled us to efficiently use numerical analysis methods. Yet analysis of turbulent flows inside the enclosure is still a challenging topic in fluid mechanics; that is because in experimental situation, it is too difficult to reach ideal adiabatic wall condition. It is at the same time difficult to measure low speeds in enclosure boundary layers through using present sensors and probes. Even numerically, although numerical methods like DES, LES and DNS have been subject to dramatic advancements, it is still nearly impossible to predict the stratification in the core of the enclosure. Non-linearity and coupling of the predominant equations have contributed into making the calculations complicated and time consuming. That is while in designing large enclosures, Rayleigh number is usually large and so, the flow nature is turbulent (Safaiy and Goshayeshi, 2010).

The aim of this study is to investigate mixed convection heat transfer inside the rectangular enclosure, the result will be compared with other investigator such as Sharif (2007) and then we continue our investigation with using Standard $k-\varepsilon$, RNG $k-\varepsilon$ and RSM Turbulent models.

MATHEMATICAL MODEL

For modeling the investigated flow, we solve continuity, momentum, energy and turbulent equations. The Prandtl number of our fluid that is water, assumed 6 and k, μ and C_p values are constant. In addition, the density is calculated while using Boussinesq approximation (Bejan, 2004). The governing equations are (Safaiy and Goshayeshi, 2011):

Continuity equation:

$$\frac{\partial u}{\partial x}+\frac{\partial v}{\partial y}=0 \tag{1}$$

X and Y momentum equations:

$$\frac{\partial u}{\partial t}+u\frac{\partial u}{\partial x}+v\frac{\partial u}{\partial y}=-\frac{1}{\rho}\frac{\partial p}{\partial x}+ \frac{\partial}{\partial x}(v+v_t)(2\frac{\partial u}{\partial x})+\frac{\partial}{\partial y}(v+v_t)(\frac{\partial u}{\partial y}+\frac{\partial v}{\partial x}) \tag{2}$$

$$\frac{\partial v}{\partial t}+u\frac{\partial v}{\partial x}+v\frac{\partial v}{\partial y}=-\frac{1}{\rho}\frac{\partial p}{\partial x}+g\beta(T-T_m)+ \frac{\partial}{\partial y}(v+v_t)(2\frac{\partial v}{\partial y})+\frac{\partial}{\partial x}(v+v_t)(\frac{\partial v}{\partial x}+\frac{\partial u}{\partial y}) \tag{3}$$

Energy equation:

$$\frac{\partial T}{\partial t}+u\frac{\partial T}{\partial x}+v\frac{\partial T}{\partial y}= \frac{\partial}{\partial x}(\frac{v}{\mathrm{Pr}}+\frac{v_t}{\sigma_T})\frac{\partial T}{\partial x}+\frac{\partial}{\partial y}(\frac{v}{\mathrm{Pr}}+\frac{v_t}{\sigma_T})\frac{\partial T}{\partial y} \tag{4}$$

The k-ε model is the most famous 2-equation model. This is because it is easy to understand and applied in programming. In k-ε Eddy-viscosity models, the turbulent field is expressed to be related to two variables: Turbulent kinetic energy transport equation:

$$\frac{\partial k}{\partial t}+u\frac{\partial k}{\partial x}+v\frac{\partial k}{\partial y}=\frac{\partial}{\partial x}(v+\frac{v_t}{\sigma_k})\frac{\partial k}{\partial x} +\frac{\partial}{\partial y}(v+\frac{v_t}{\sigma_k})\frac{\partial k}{\partial y}+P_k+G_k-\varepsilon \tag{5}$$

Dissipation of 'turbulent kinetic energy transport' equation:

$$\frac{\partial \varepsilon}{\partial t}+u\frac{\partial \varepsilon}{\partial x}+v\frac{\partial \varepsilon}{\partial y}=\frac{\partial}{\partial x}(v+\frac{v_t}{\sigma_\varepsilon})\frac{\partial \varepsilon}{\partial x}$$
$$+\frac{\partial}{\partial y}(v+\frac{v_t}{\sigma_\varepsilon})\frac{\partial \varepsilon}{\partial y}+C_1\frac{\varepsilon}{k}P_k+ \quad (6)$$
$$C_2\frac{\varepsilon^2}{k}+C_3\frac{\varepsilon}{k}G_k-R_\varepsilon$$

The Eddy viscosity from Prandtl-Kolmogorov relation is achieved:

$$v_t=C_\mu f_\mu\frac{k^2}{\varepsilon} \quad (7)$$

The 'stress production term', P_k, can also be achieved by:

$$P_k=v_t\left[2\left(\frac{\partial u}{\partial x}\right)^2+2\left(\frac{\partial v}{\partial x}\right)^2+\left(\frac{\partial u}{\partial y}+\frac{\partial v}{\partial y}\right)^2\right] \quad (8)$$

The 'buoyancy term', G_k can be expressed as follows:

$$G_k=-g\beta\frac{v_t}{\sigma_t}\frac{\partial T}{\partial y} \quad (9)$$

Also for term of R_ε in ε equation, we have:

$$R_\varepsilon=\frac{C_\mu\rho\eta^3\left(1-\frac{\eta}{\eta_0}\right)}{1+\beta\eta^3}\frac{\varepsilon^2}{k} \quad (10)$$

$$\eta=\frac{Sk}{\varepsilon} \quad (11)$$

The major difference between standard $k-\varepsilon$ and RNG $k-\varepsilon$ is in the term of R_ε in dissipation of turbulent kinetic energy transport equation. In the other words, the RNG $k-\varepsilon$ model is the same with standard $k-\varepsilon$, but the standard $k-\varepsilon$ can be achieved by experimental but the Prandtl number has improved for turbulent RNG $k-\varepsilon$ model. In the RSM model, calculation of each Reynolds stresses terms is done with the aid of a transport equation. To solve a two-dimensional problem we need to solve four transport equations. Otherwise, if you resort to a 2-equation model such as k-ε, you should only suffice to finding just two of the unknown variables with a good approximation and the rest will be calculated less precisely. This model could include many of complex effects of flows in the nature and the engineering. Among them we can point out to the natural convection flows or buoyancy flows both of which we can be efficiently modeled using this model. For RSM model, the turbulence equations are as follows: Reynolds stress transport equations:

$$\frac{D}{Dt}\left(\overline{u_i'u_j'}\right)=\frac{\partial\left(d_{ijk}\right)}{\partial x_k}+P_{ij}+G_{ij}+\phi_{ij}-\varepsilon_{ij} \quad (12)$$

That:

$\frac{D}{Dt}\left(\overline{u_i'u_j'}\right)=\frac{\partial\left(\overline{u_i'u_j'}\right)}{\partial t}+\bar{u}_k\frac{\partial\left(\overline{u_i'u_j'}\right)}{\partial x_k}$: Advection (by mean flow)

$d_{ijk}=v\frac{\partial\left(\overline{u_u'u_j'}\right)}{\partial x_k}-$
$\overline{\frac{P'}{\rho}\left(u_i'\delta_{jk}+u_j'\delta_{ik}\right)}-\overline{u_i'u_j'u_k'}$: Diffusion

$P_{ij}=-\left[\left(\overline{u_i'u_k'}\right)\frac{\partial\bar{u}_j}{\partial x_k}+\left(\overline{u_j'u_k'}\right)\frac{\partial\bar{u}_i}{\partial x_k}\right]$: Production (by mean strain)

$G_{ij}=\left(\overline{u_i'f_j'+u_j'f_i'}\right)$: Production (by body force)

$\phi_{ij}=\overline{\frac{P'}{\rho}\left(\frac{\partial u_i'}{\partial x_j}+\frac{\partial u_j'}{\partial x_i}\right)}=\overline{\frac{2P'}{\rho}S_{ij}}$: Pressure-strain correlation

$\varepsilon_{ij}=2v\overline{\frac{\partial u_i'}{\partial x_k}\frac{\partial u_j'}{\partial x_k}}$: Dissipation

Turbulent kinetic energy transport equation:

$$\frac{Dk}{Dt}=\frac{\partial d_i^{(k)}}{\partial x_i}+P^{(k)}+G^{(k)}-\varepsilon \quad (13)$$

Except the terms convection and production in Reynolds stress transport equation, all the other terms have contributed in introducing a series of correlations, which have to be identified according to some known and unknown quantities so that the equation system can be configured. Diffusion term:

$$-\overline{u_i'u_j'u_k'}=C_S\frac{k}{\varepsilon}\overline{u_k'u_l'}\frac{\partial\overline{u_i'u_j'}}{\partial x_l} \quad (14)$$

Redistribution term:

$$\phi_{ij}=\phi_{ij}^{(1)}+\phi_{ij}^{(2)}+\phi_{ij}^{(w)} \quad (15)$$

Table 1. Coefficients for RNG k-ε turbulent model.

C_μ	0.0845
σ_k	1
σ_ε	1.3
C_1	1.42
C_2	1.68
η_0	4.38
β	0.012
K	0.41

Table 2. Coefficients for standard k-ε turbulent model.

C_μ	0.0845
σ_k	1
σ_ε	1.3
C_1	1.42
C_2	1.68

Table 3. Coefficients for RSM turbulent model.

$c_2^{(w)}$	0.3
$c_1^{(w)}$	0.5
C_s	0.22
C_1	1.8
C_2	0.6
C_3	2.5

That:

$$\phi_{ij}^{(1)} = -C_1 \frac{\varepsilon}{k}\left(\overline{u_i' u_j'} - \frac{2}{3}k\delta_{ij}\right)$$

$$\phi_{ij}^{(2)} = -C_2\left(P_{ij} - \frac{1}{3}P_{kk}\delta_{ij}\right) \quad (16)$$

$$\phi_{ij}^{(w)} = \left(\tilde{\phi}_{kl} n_k n_l \delta_{ij} - \frac{3}{2}\tilde{\phi}_{ik} n_j n_k - \frac{3}{2}\tilde{\phi}_{jk} n_i n_k\right)\psi$$

$$\tilde{\phi}_{ij} = -C_1^{(w)} \frac{\varepsilon}{k}\overline{u_i' u_j'} + C_2^{(w)}\phi_{ij}^{(2)}$$

$$\psi = \frac{k^{\frac{3}{2}}/\varepsilon}{C_3 y_n}$$

y_n is the distance from the wall. The role of terms $\Phi_{ij}^{(2)}$, $\Phi_{ij}^{(1)}$ is to return isotropy (or terminating anisotropic flow with distributing kinetic energy of Reynolds huge stresses among the stresses of smaller size). The terms $\Phi_{ij}^{(1)}$ and $\Phi_{ij}^{(2)}$ are called "return to isotropy" and "isotropization of production", respectively. The term $\Phi_{ij}^{(w)}$ is named as "wall reflection term". For dissipation term, we have:

$$\varepsilon_{ij} = \frac{2}{3}\delta_{ij}\varepsilon \quad (17)$$

The constants of the aforementioned equations can be found in Tables 1, 2 and 3. For solving the governing equations we use the 'finite volume method' which has been explains in Patankar (2003) and Safaiy (2009). This method is a specific case of residual weighting methods. In this approach, the computational field is divided to some control volumes in a way that a control volume surrounds each node and control volumes have no volumes in common. Then, the differential equation is integrated on each control volume. Profiles in pieces that show changes (of a certain quantity like temperature, velocity, etc.) among the nodes are used to calculate the integrals. The result is discretization equation, which includes quantities for a group of nodes (Safaiy and Goshayeshi, 2011). The advantage of this method is high accuracy even in low nodes. The Ra is changing from 10^5 to 10^7 for laminar flow and 6×10^9 for turbulent flow. Figure 1 is the schematic of this study. In these conditions, stream function is:

$$u = \frac{\partial \psi}{\partial y} \quad v = -\frac{\partial \psi}{\partial x} \quad (18)$$

MESH INDEPENDENCY

Meshes that designed to cover control volumes are square meshes provided on physical domain with different distances in order to reach independence. The mentioned mesh-independence for each turbulence model and any different Ri has been separately calculated. Tables 4 to 6 show some meshes used in this study.

RESULTS

In this study, we investigate the mixed convection inside the rectangular enclosure with moving wall. The main dimensionless parameter in this investigation is Richardson number that varies from 0.1 to 10. Figures 2 to 5 show

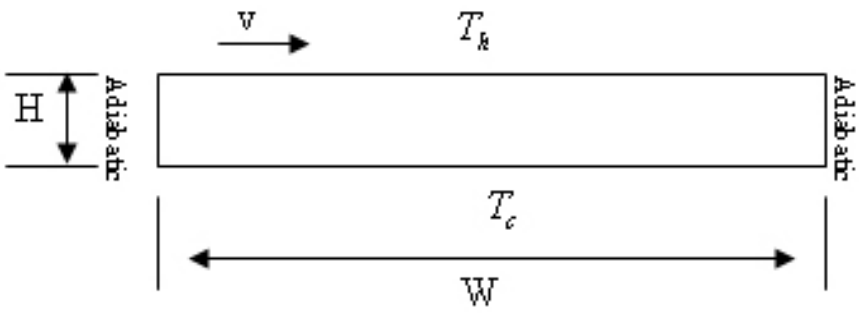

Figure 1. Schematic of the problem.

Table 4. Some meshes used for solving the problem with standard k-ε model.

Ri	Standard k-ε		
Ri = 0.1	570 × 57	1010 × 101	1610 × 161
Ri = 1	680 × 68	1350 × 135	2010 × 201
Ri = 10	750 × 75	1500 × 150	2250 × 225

Table 5. Some meshes used for solving the problem with RNG k-ε model.

Ri	RNG k-ε		
Ri = 0.1	610 × 61	1190 × 119	1810 × 181
Ri = 1	810 × 81	1600 × 160	2410 × 241
Ri = 10	900 × 90	1750 × 175	2700 × 270

Table 6. Some meshes used for solving the problem with RSM model.

Ri	RSM		
Ri = 0.1	750 × 75	1190 × 119	2010 × 201
Ri = 1	900 × 90	1600 × 160	2700 × 270
Ri =10	1050 × 105	1800 × 180	3000 × 300

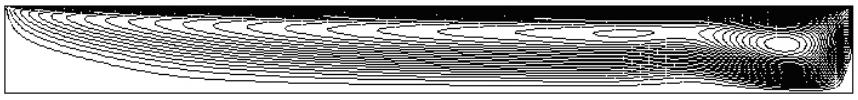

Figure 2. Contours of Stream Function for $Ra = 10^5$ and $Ri = 0.1$.

Figure 3. Contours of Isotherm Lines for $Ra = 10^5$ and $Ri = 0.1$.

Figure 4. Contours of stream function for $Ra = 10^6$ and $Ri = 1$.

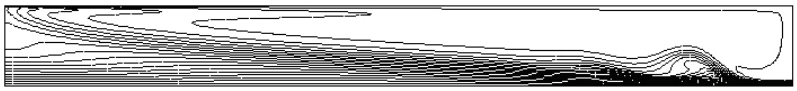

Figure 5. Contours of isotherm lines for $Ra = 10^6$ and $Ri = 1$.

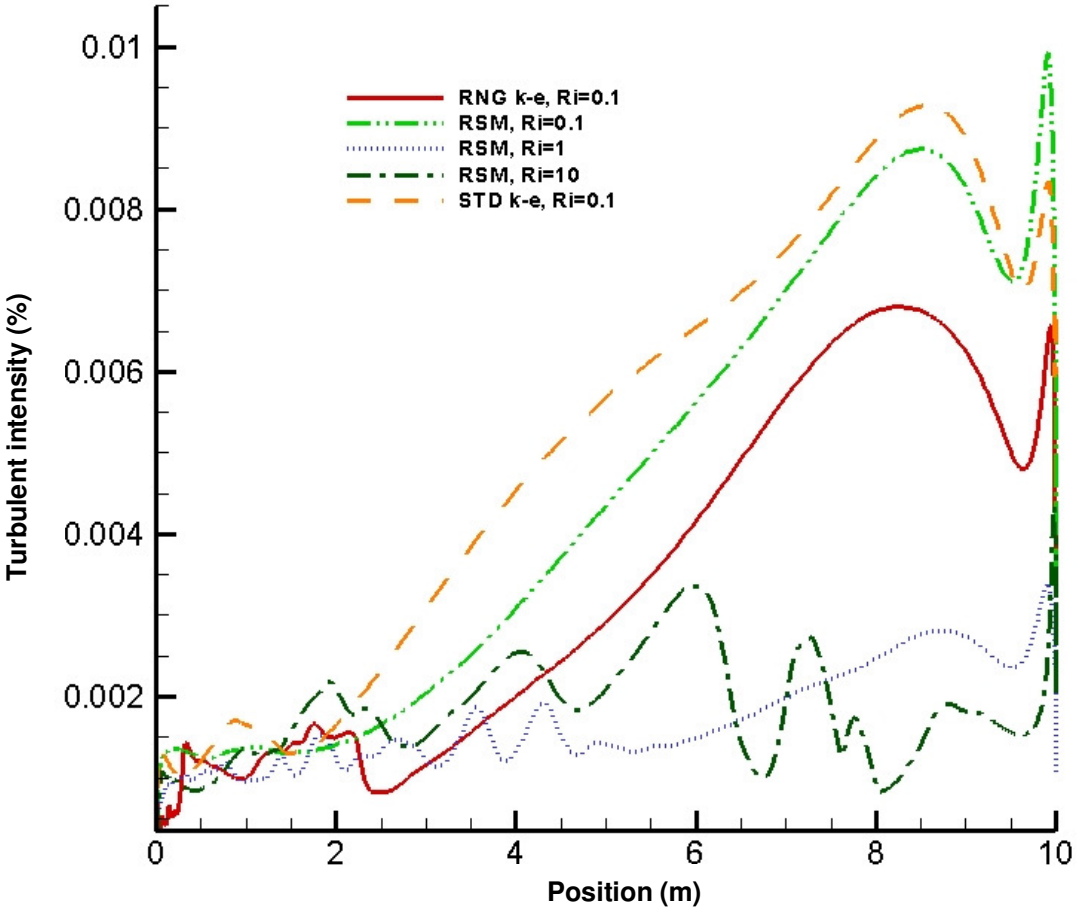

Figure 6. Turbulent intensity diagram at y/H = 0.5 and different turbulent models.

the 'stream function' and 'isotherm line' for laminar flow and Figure 17 shows changing of Local Nusselt number in cold and hot walls in Ri = 1 at comparison of result of Sharif (2007). Good agreement was found in contours and diagrams. Turbulence intensity (Figure 6) is defined by fluctuation velocity (U') divided by average flow velocity (U_{ave}).

$$\tilde{\varsigma} = \frac{\left[\left(u'^2\right)\right]^{\frac{1}{2}}}{\bar{u}} = \frac{\left[\frac{1}{T}\int_0^T u'^2 dt\right]^{\frac{1}{2}}}{\bar{u}} \quad (19)$$

Turbulence intensities are considered small if less than

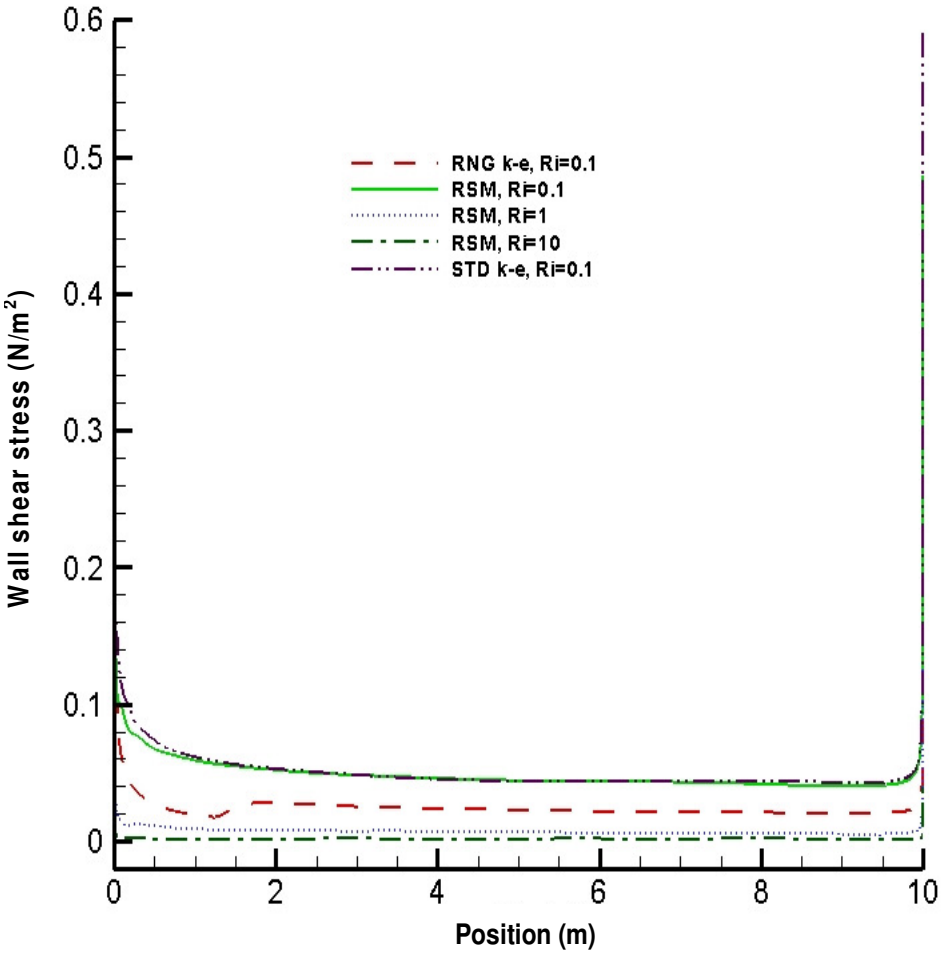

Figure 7. Shear stress curve on the hot upper wall for different Richardson numbers and turbulent models.

1% and big if more than 10%. The figure well demonstrates that the 'turbulence intensity' is relatively low inside the enclosure. In addition, the curve shows that the minimum value of turbulence intensity corresponds to the left wall and its maximum value happens inside the boundary layer on the right wall. Although the turbulence intensity is maximum at Ri = 0.1, there occurs maximum fluctuation and minimum value for turbulence intensity at Ri = 10. The reason is the existence of small but numerous eddies at the state of natural convection. Whilst at forced convection, one giant and strength full eddy occupies the whole enclosure. Figure 7 demonstrate the Shear stress curve on the hot upper wall. As seen from the curve, the shear stress value is rather steady in every Richardson except at both extremes near the left and the right walls. It is also understood from the curve that the shear stress is minimum at Ri = 10 and maximum at Ri = 10. In a way, that at natural convection, the stress neighbors zero. The UU, VV, WW and UV Reynolds stresses are shown in various Richardson's and for the RSM turbulent model. It is obvious from Figures 8 to 11 that the UU, VV and WW curves bear a similarity in shape and have the same maximum points. However, the UV curve stands out. It is also evident that the curves 8 to 10 at Ri = 0.1 grow rather exponentially from the left wall until they reach to their peak value in x~8.5 m. Then, decline down to the footsteps of the boundary layer after which they increase up to the vicinity of the right wall. On the right wall, again the Reynolds stresses fall to zero due to validity of the 'no slip condition'. For the mixed convection, the Reynolds stresses are all –except at some points- somewhat near zero forming a straight line on the curve. It only rises slightly at the footsteps of the boundary layer of the right wall and falls again to zero on the wall itself. For Ri = 10, though the stresses are less stable as the Reynolds stresses curve fluctuates. This is due to both the impacts of Buoyancy force and to the properties of 'natural convection' at this Richardson. The case is different for UV stress.

At Ri = 0.1, the curve plummets rather exponentially from zero until it attains the minimum value at x~8.4.

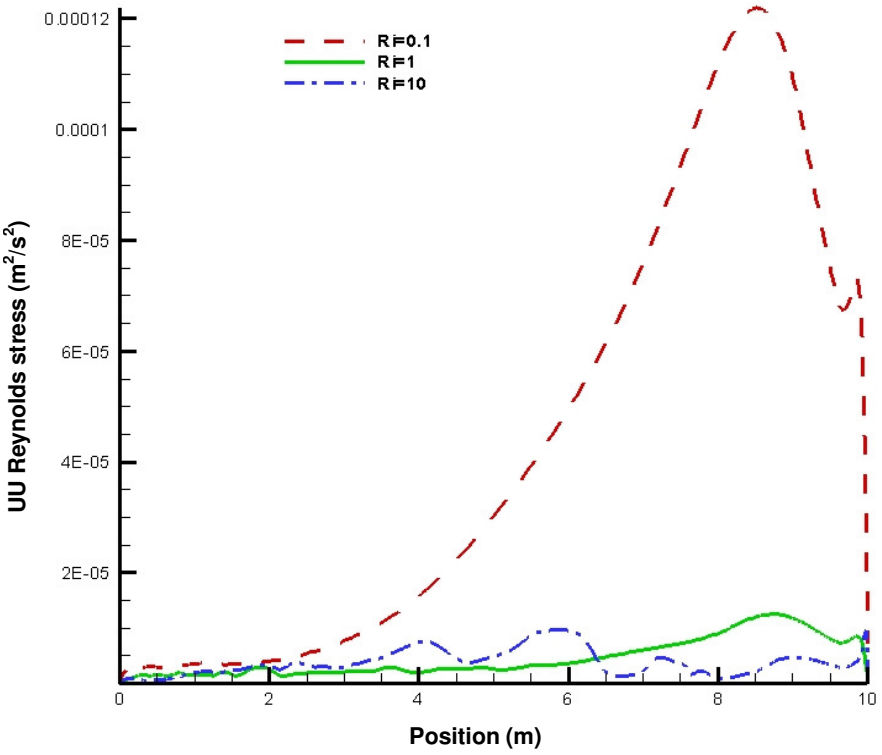

Figure 8. UU Reynolds stress diagram at y/H = 0.5.

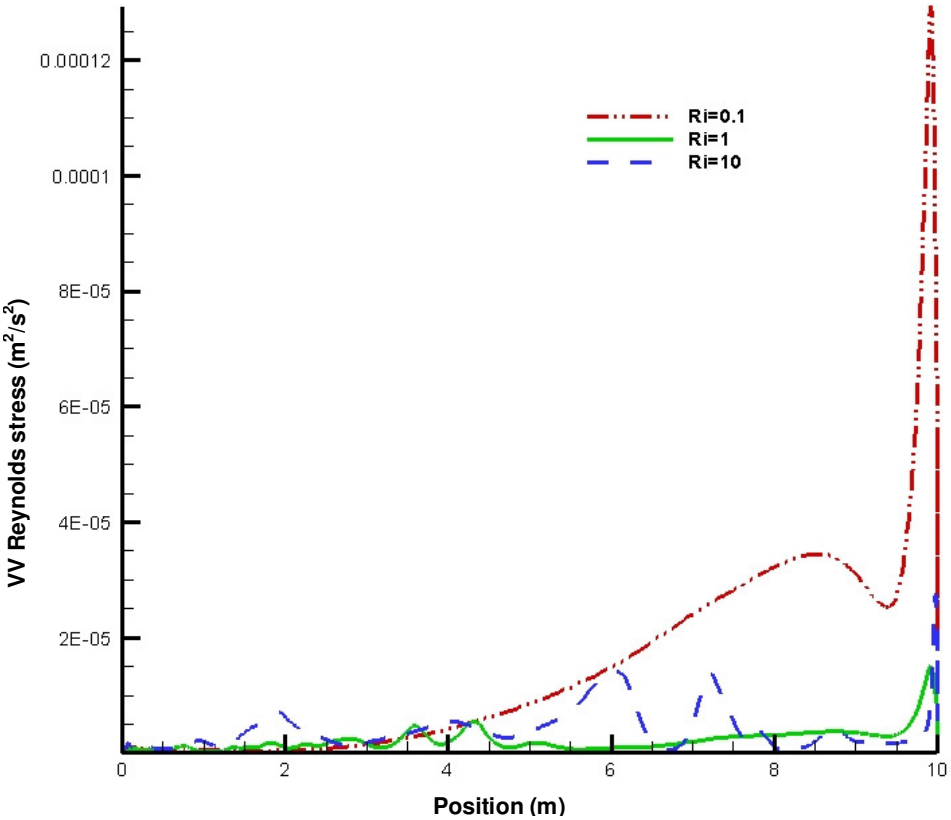

Figure 9. VV Reynolds stress diagram at y/H = 0.5.

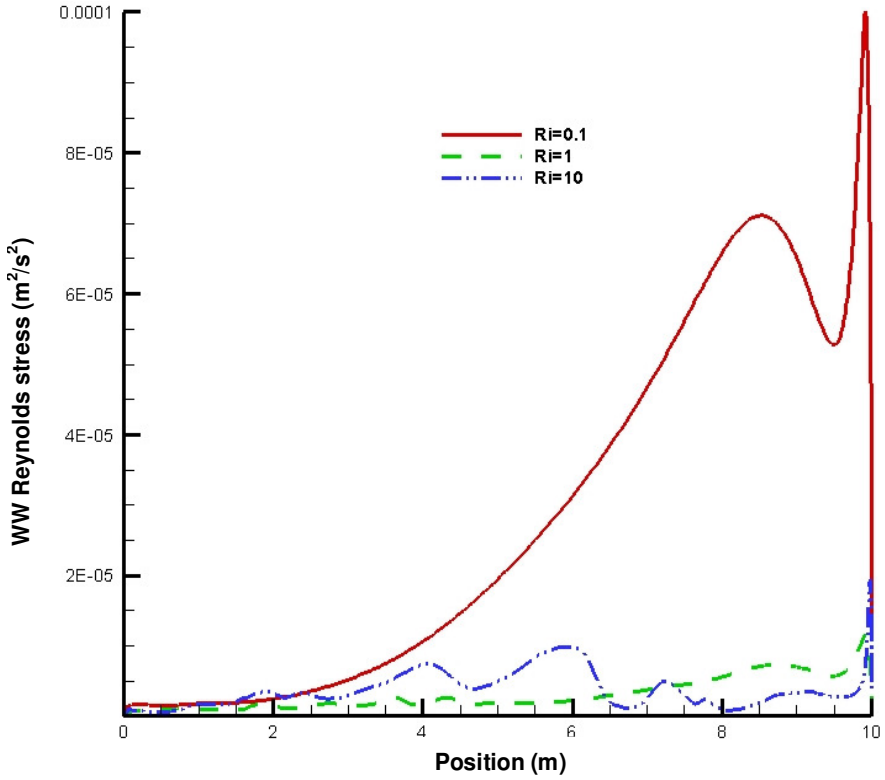

Figure 10. WW Reynolds stress diagram at y/H = 0.5.

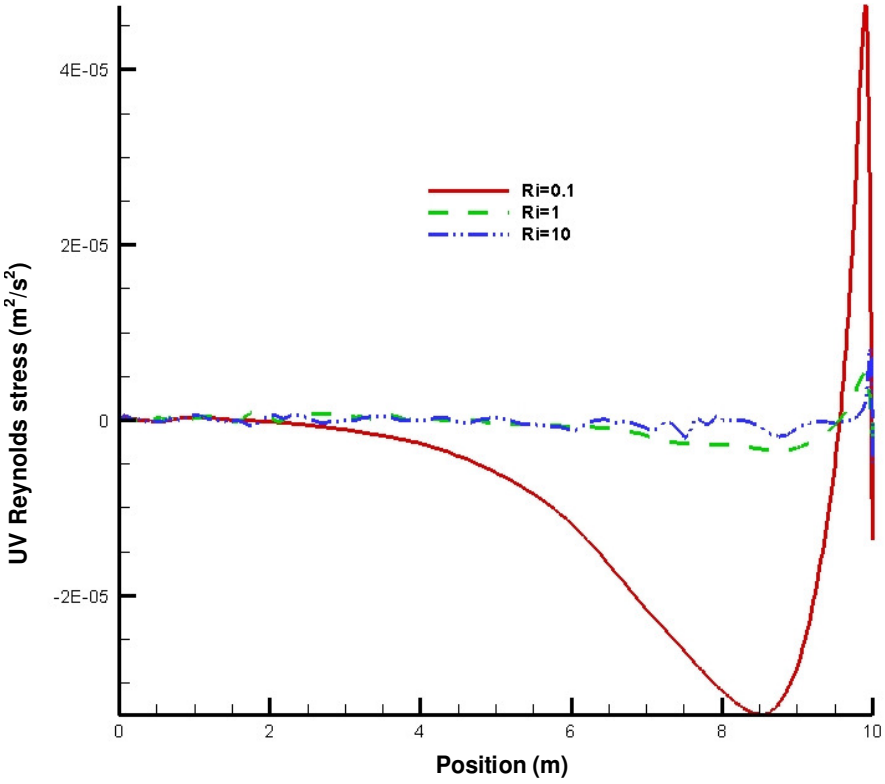

Figure 11. UV Reynolds stress diagram at y/H = 0.5.

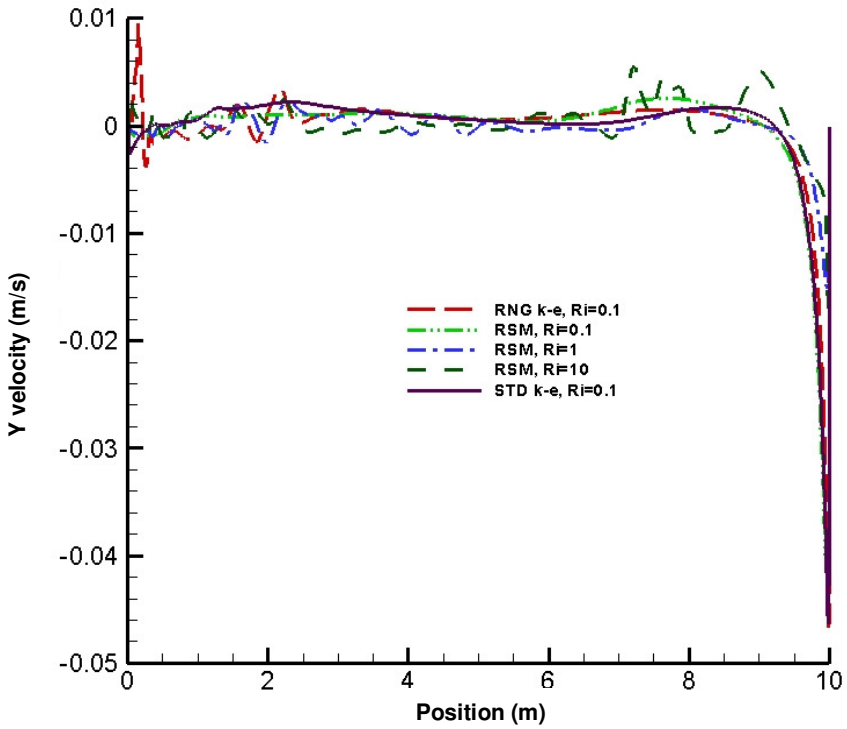

Figure 12. Vertical velocity diagram at y/H = 0.5.

From there after it goes, upwards to touch the maximum value in the cold wall is round about it. The UV stress is again zero on the cold wall itself. At Ri = 1, the UV Reynolds stress, except at some points, forms a straight line with values near zero. The aforementioned values are negative at the interval between 6.5 and 9 m. At Ri = 10, the UV Reynolds stress has inherent vacillating characteristics, yet the significance of the fluctuations are much less than the fluctuations of UU, VV and WW Reynolds stresses. The diagram of V in terms of the position at the mid height is drawn in Figure 12 for a variety of Richardson numbers and turbulence models. As seen in the figure, at Ri = 0.1, the size of V barely changes from zero. Only in two small areas on the two end of the wall where the curve is subject to a maximum and minimum. At Ri = 10, the velocity is no more equal to zero except at a number of points. Furthermore, the 'max and min' values of both ends undergo a short fall. Also the shape of the curve at this state and between x = 7.3 m and x = 9.3 m is subject to some upward leaps. Therefore, it can be inferred that as Ri grows, the changes in velocity grow and there is more fluctuation. Such happening is justifiable according to the streamlines. The upper wall's speed downturn and the consequent raise in Ri initiates the formation of some separate vortexes inside the enclosure; something that explains the abundant fluctuations of the V profile. This is even truer at Ri = 10. Figure 13 depicts the Local Nusselt number curve on the hot upper wall for different Richardson numbers and turbulence models. As it is observed from the figure, the maximum local Nusselt is around x = 0, but as x grows to the end of the wall, the value declines to zero. The local Nusselt number drops sharply with a high gradient in the beginning but it continues with a much lower one. If we raise the Ri, -Ri = 10- the Nusselt number's max value drops significantly and as X grows, it falls again but with a difference which is the curve takes some upward leaps-but still keeps its decreasing path- along the wall before it reaches its minimum at the end of the wall.

Also it is clear from the aforementioned chart that the Nusselt number enjoys maximum value under the forced convection and minimum value under the natural convection, all of which shows that under equal circumstances forced convection has a higher heat transfer rate. It can also be said that due to a greater mixing at the turbulent state, the heat transfer rate is generally higher than the laminar state. Figure 18 represents the turbulent kinetic energy curve (K) on the top and bottom walls at Ri = 1 and according to Standard K turbulence model. Apparently this energy is quite symmetrical on the hot and cold planes and thereby the K enjoys a balanced value at Ri = 1. Figure 14 is a Contour related to this curve bearing the proof to the aforementioned words. This is not true at Ri = 0.1 though, as Figures 15 and 16 show. Due to the impact of the upper wall's velocity, the turbulent kinetic energy tends to the left side of the hot wall where the velocity enters the

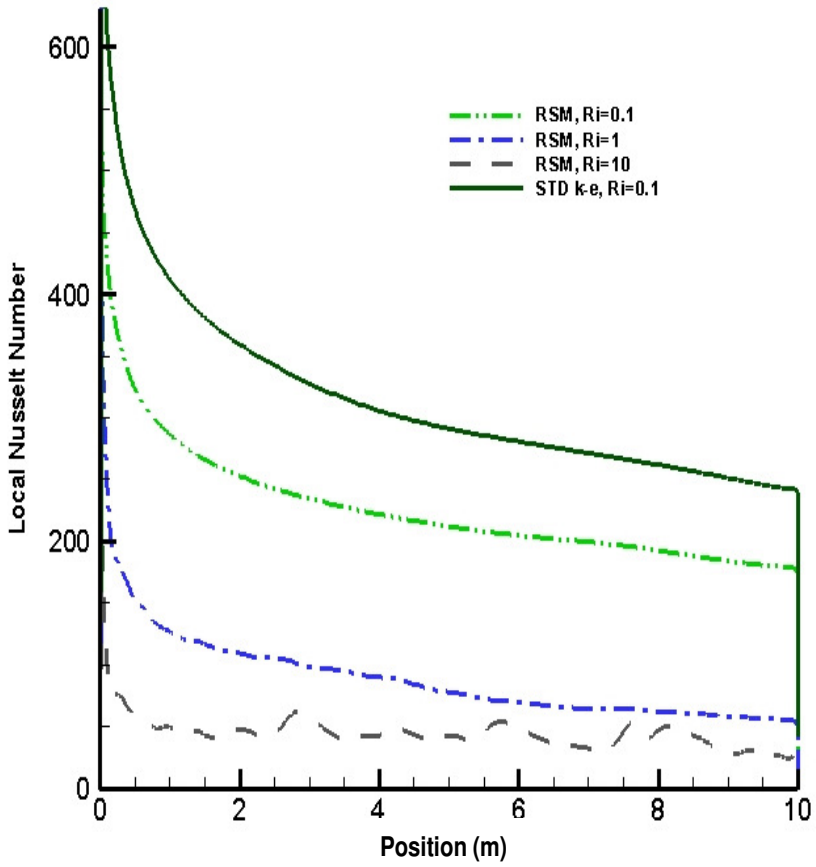

Figure 13. Local Nusselt number diagram on the hot upper wall for different Richardson numbers.

Figure 14. Contour of turbulent kinetic energy at Ri = 1 and for $k-\varepsilon$ Standard turbulent model.

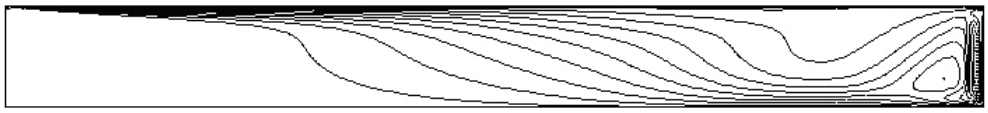

Figure 15. Contour of turbulent kinetic energy at Ri = 0.1 and for RNG $k-\varepsilon$ turbulent model.

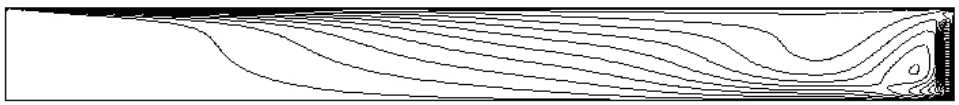

Figure 16. Contour of turbulent kinetic energy at Ri = 0.1 and for standard $k-\varepsilon$ turbulent model.

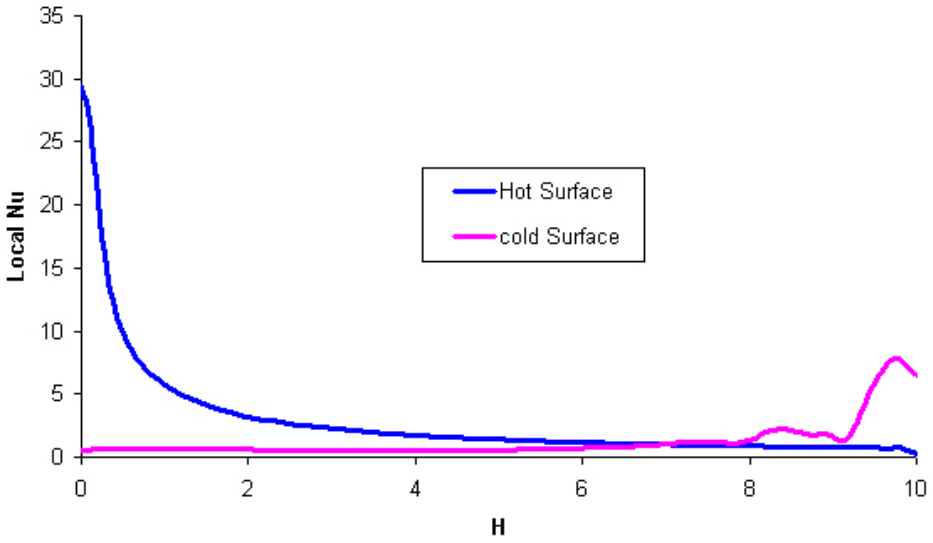

Figure 17. Variation of the local Nusselt number along the hot and cold surfaces, Laminar flow and Ri = 1.

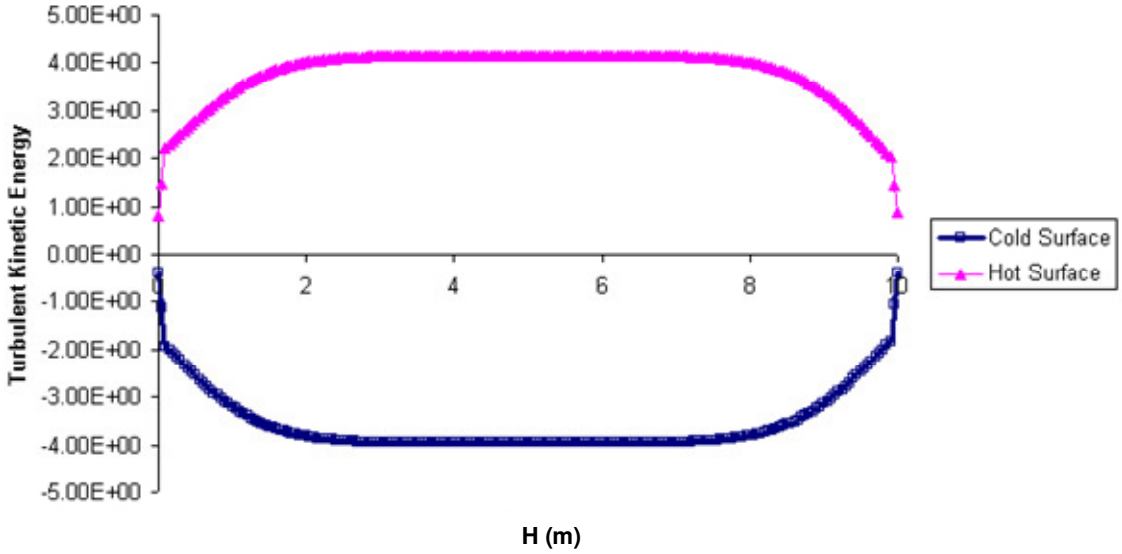

Figure 18. Diagram of turbulent kinetic energy at Ri = 1, on the top and bottom walls and for standard $k-\varepsilon$ turbulent model.

enclosure. This means that the K is maximum at the entrance of velocity to the enclosure.

CONCLUSIONS

In this study, turbulence mixed convection in water-filled enclosures was 'modeling numerically' by finite volume method for different Richardson numbers. Initially and to prove the validity of the results, stream function and temperature contours have been compared to the laminar results driven from the research (Sharif, 2007) and after the accuracy of the calculations is attested, the case is solved with RNG $k-\varepsilon$, standard $k-\varepsilon$ and RSM turbulence models. The results testify that:

i) The value of turbulence intensity is maximum under forced convection and it bears the most fluctuations and the least value under natural convection.
ii) With Richardson number growing, velocity variance

grows vertically and fluctuations are seen in it.
iii) At Ri = 10, the Reynolds stresses curve has numerous fluctuations all of which is the impact of the 'buoyancy force' and the properties of the natural convection at this Richardson.
iv) At the turbulent state, due to a greater mixing, the heat transfer rate is generally higher than the laminar state.
v) The Nusselt number enjoys maximum value under the forced convection and minimum value under the natural convection.
vi) Standard $k-\varepsilon$, RNG $k-\varepsilon$ and RSM have good agreement between their results, although RSM turbulent model is more accurate and time consuming.

Nomenclature: u,v**,** velocities in x and y directions (m/s); x,y**,** Cartesian coordinates (m); P**,** pressure (Pa); T**,** temperature (K); **t,** time (s); **g,** gravitational acceleration (m/s^2); **K,** turbulent kinetic energy transport (m^2/s^2); k**,** thermal conductivity (W/m.K); **Re,** Reynolds number; **Ri,** Richardson number; **Gr,** Grashof number; **Nu,** Nusselt number; **Pr,** Prandtl number; **Ra,** Rayleigh number.

Greek symbols: ε**,** dissipation of turbulent kinetic energy transport (m^2/s^3); υ_t**,** turbulent kinematics viscosity (m^2/s); σ_T**,** turbulent thermal diffusivity (m^2/s); β**,** thermal expansion coefficient (1/K); ρ**,** density (Kg/m^3); υ**,** kinematics viscosity (m^2/s]).

Subscripts: h, hot wall; **c,** cold wall; **m,** mean; **lid,** Lid.

REFERENCES

Basak T, Roy S, Sharma PK, Pop I (2009). Analysis of Mixed Convection Flows within a Square Cavity with Uniform and Non-Uniform Heating of Bottom Wall. Int. J. Therm. Sci., 48(5): 891-912.

Bejan A (2004). Convection heat transfer. A Wiley-Interscience publication. John Wiley, New York.

Oztop HF, Dagtekin I (2004). Mixed Convection In Two-Sided Lid-Driven Differentially Heated Square Cavity. Int. J. Heat Mass Trans., 47: 1761-1769.

Patankar SV (2003). Numerical Heat Transfer and Fluid Flow. Translated by: Dr. M. Moghiman. Ferdowsi University Press, [in Farsi].

Rahman MM, Alim MA, Mamun MA H and et. al. (2007). Numerical Study of Opposing Mixed Convection in a Vented Enclosure. ARPN J. Eng. Appl. Sci., 2: 25-35.

Safaiy MR (2009). The Study of Turbulence on Mixed Convection Heat Transfer in Newtonian and Non-Newtonian Fluids inside Rectangular Enclosures in Different Richardson Numbers. M. Sc. Thesis. Islamic Azad University-Mashhad Branch, Iran, (in Farsi Language).

Safaiy MR, Goshayeshi HR (2011). Investigation of turbulence mixed convection in air-filled enclosures. J. Chem. Eng. Mat. Sci., 2(6): 87-95.

Safaiy MR, Goshayeshi HR (2010). Numerical Simulation of Laminar and Turbulence Flow of Air: Natural & Mechanical Ventilation inside a Room. 10th REHVA world congress; Clima 2010: Sustainable Energy Use in Buildings. Antalya, Turkey.

Saha S, Mamun AH, Hossain M Z, Islam AKMS (2008). Mixed Convection in an Enclosure with Different Inlet and Exit Configurations. J. Appl. Fluid Mech., 1: 78-93.

Saha S, Saha G, Ali M, Islam Md Q (2006). Combined Free and Forced Convection inside a Two-Dimensional Multiple Ventilated Rectangular Enclosure. ARPN J. Eng. Appl. Sci., 1: 23-35.

Sharif MAR (2007). Laminar mixed convection in shallow inclined driven cavities with hot moving lid on top and cooled from bottom. Appl. Therm. Eng., 27: 1036-1042.